

PCCP

Accepted Manuscript



This is an *Accepted Manuscript*, which has been through the Royal Society of Chemistry peer review process and has been accepted for publication.

Accepted Manuscripts are published online shortly after acceptance, before technical editing, formatting and proof reading. Using this free service, authors can make their results available to the community, in citable form, before we publish the edited article. We will replace this *Accepted Manuscript* with the edited and formatted *Advance Article* as soon as it is available.

You can find more information about *Accepted Manuscripts* in the [Information for Authors](#).

Please note that technical editing may introduce minor changes to the text and/or graphics, which may alter content. The journal's standard [Terms & Conditions](#) and the [Ethical guidelines](#) still apply. In no event shall the Royal Society of Chemistry be held responsible for any errors or omissions in this *Accepted Manuscript* or any consequences arising from the use of any information it contains.

"Tschitschibabin type Biradicals": Benzenoid or Quinoid?

Cite this: DOI: 10.1039/x0xx00000x

Prince Ravat^a, and Martin Baumgarten^{a*}Received 00th January 2014,
Accepted 00th January 2014

DOI: 10.1039/x0xx00000x

www.rsc.org/

Our findings provide a better understanding of the discrepancies related to the discussion in the literature on the ground state of Tschitschibabin's hydrocarbon. A series of phenylene bridged bisnitroxide molecules were designed and studied for the comparison. The simple theoretical and experimental methodologies have been developed and utilized to understand the singlet biradicaloids which exist in semi-quinoid form and exhibits characteristics of biradicaloid and quinoid form simultaneously.

Introduction

Shortly after the discovery of the first stable organic radical, namely triphenylmethyl by Gomberg,¹ Tschitschibabin reported the synthesis of the first biradical linked through biphenyl bridge in 1907, now more commonly known as Tschitschibabin's hydrocarbon (HC) or biradical.² Recently there is a considerable amount of interest of various research groups in synthesizing Kekulé open shell polyaromatic HC owing to their application in designing spintronic and energy storage devices.³⁻⁷ In most of the cases the molecular structural design of Kekulé open shell polyaromatic hydrocarbons relied on the bases of Tschitschibabin's HC, and the biradicaloid nature of HC appeared as a consequence of loss of quinoidal form upon extending conjugation thereby gaining the aromaticity.⁸⁻¹² As the Tschitschibabin's HC is a fundamental building block in designing the majority of Kekulé open shell polyaromatic HCs, it has been extensively studied by various EPR spectroscopic techniques and theoretical calculations.¹³ While Thiele's HC¹⁴ was well accepted as quinoid singlet, there are different opinions on the ground state of Tschitschibabin's HC, whether it is open shell or closed shell (Figure 1).¹⁵ In principle the EPR spectroscopy should be able to resolve this problem simply but the analysis of this molecule is severely affected by paradox, disputation and repugnancies.¹⁶⁻²⁰ Firstly Reitz and Weissman investigated Tschitschibabin's HC, labeled at exocyclic carbon atom with ¹³C.¹³ They obtained EPR spectra corresponding to two non-interacting triphenyl methyl moieties with $J < 10^8$ Hz.¹⁹ This result showed the divergence with the initial theoretical study which predicted the $J > 10^{13}$ Hz.^{21, 22} This discrepancy often alluded as "biradical paradox".^{16, 23, 24} Later several theories have been proposed relating to the biradical paradox of this molecule. In subsequent years the studies by Brauer *et al.*,^{23, 25} van der Hart, and Oosterhoff²⁶ suggested that the biradical paradox of Tschitschibabin's HC is not real and the observed EPR spectra, alike the doublet species, is due to impurities owing to its high reactivity. Brauer *et al.* did extensive ENDOR studies and suggested that the spectrum originated from a monoradical impurity with structural formula shown in Figure 2a.^{23, 25} Along with this van der Hart and Oosterhoff suggested dimers of the

biradicals (Figure 2b), responsible for the observed EPR spectrum.²⁶ Thus the reported EPR spectrum with vanishing exchange interactions ($J < 10^8$ Hz) could be imputed to impurities thereby solving the biradical paradox of Tschitschibabin's HC. This problem seemed to be completely resolved when Brauer *et al.* reported the triplet resonance signal for the polycrystalline sample of Tschitschibabin's HC.^{17, 18} But the discrepancies were triggered back when Montgomery *et al.* successfully obtained the single crystal of Tschitschibabin's HC, which provided doublet EPR spectrum alike all previous studies of the same.²⁰ Since then no clear explanation has been given to such conflicting observations which were supposedly caused by the possibility of the paramagnetic impurities.

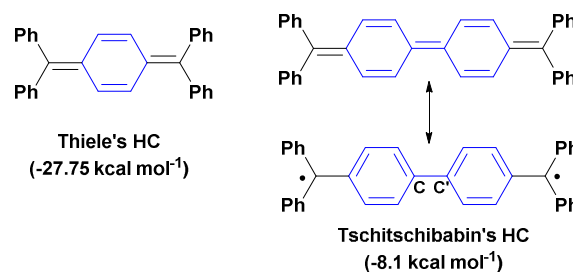


Figure 1. Thiele's and Tschitschibabin's hydrocarbon and calculated singlet-triplet energy gap.

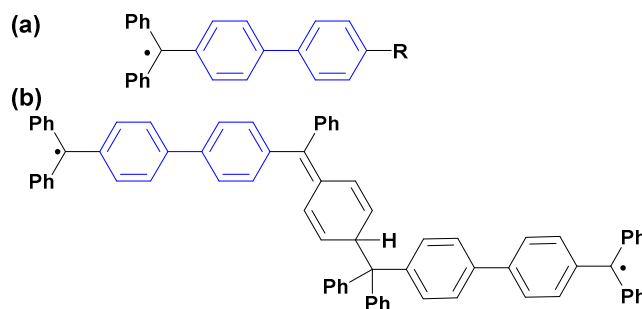


Figure 2. (a) Structural formula of monoradical impurity proposed by Brauer *et al.* (b) structural formula of dimer impurity proposed by van der Hart and Oosterhoff.

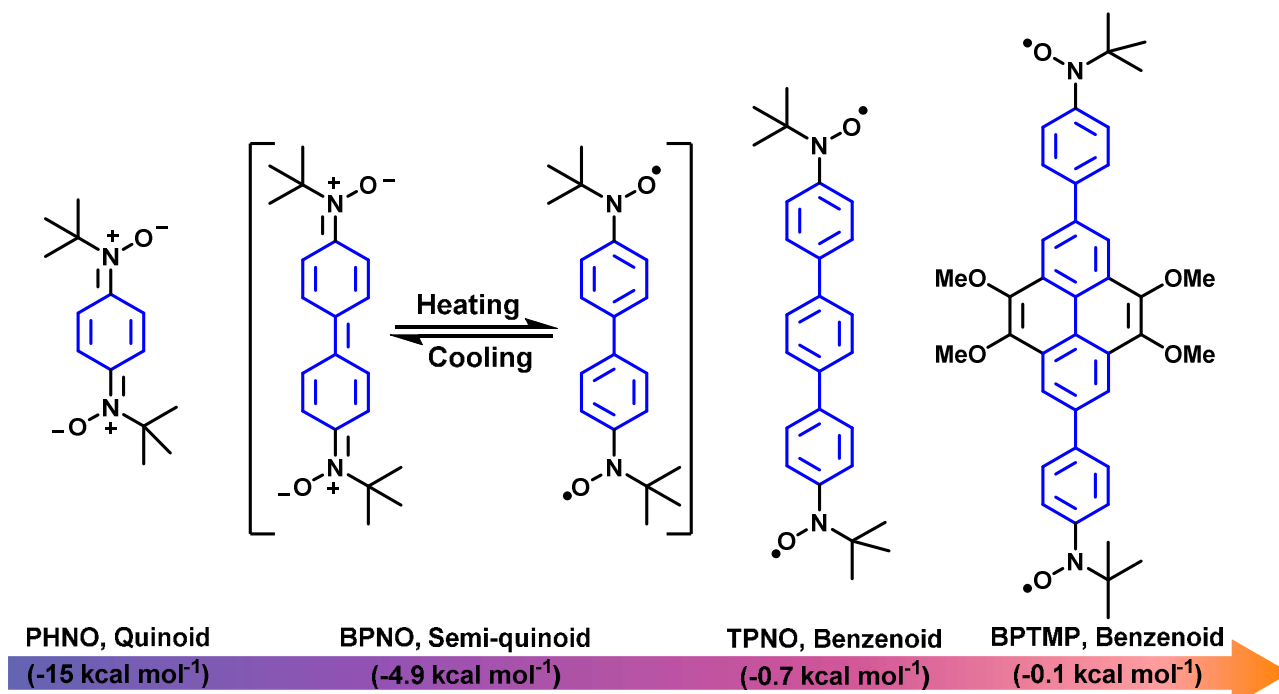
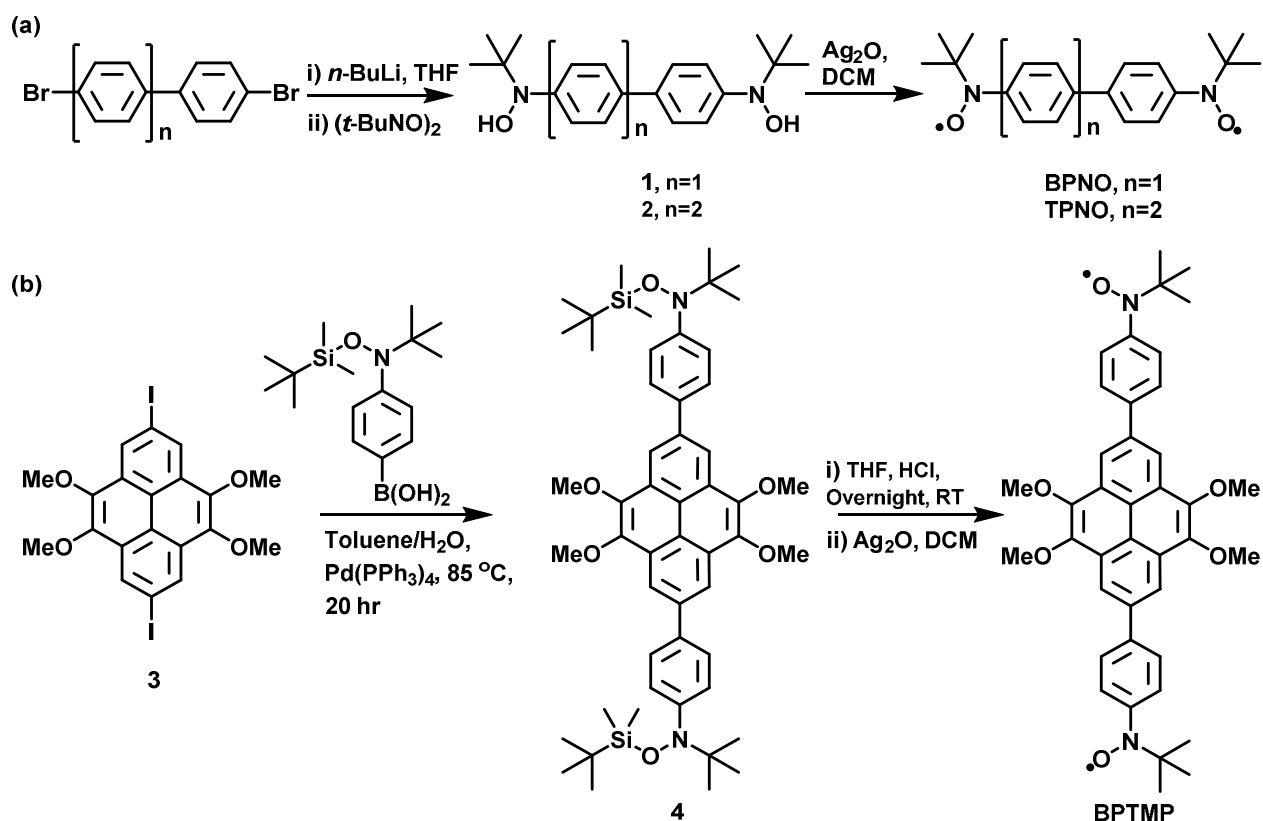


Figure 3. The structures of molecules under investigation and the calculated energy gap between singlet and triplet states.

Serendipitously during the course of our study on organic biradical systems for the Bose-Einstein condensation we found the molecule BPNO (N,N'-([1,1'-biphenyl]-4,4'-diyl)bis(N-(tert-butylaminoxyl)) which exists in semi-quinoid form (Figure 3).²⁷⁻²⁹ At room temperature BPNO showed doublet EPR spectrum. Even after several purifications by column followed by repetitive crystallization no improvement in EPR spectrum was observed. Thus this molecule was studied in depth by variable temperature EPR, UV-Vis spectroscopy and DFT calculation. All the analysis led to inference that the molecule BPNO exists in semi-quinoid form with very large singlet-triplet energy gap (ΔE_{ST}) of -5.1 kcal mol⁻¹. A similar semi-quinoid structure was also found for the 2,7-disubstituted tetramethoxyppyrene based biradical system.³⁰ The initially observed monoradical like spectrum at room temperature was caused by the trace amount of mono radical impurity and the very weak intensity biradical spectrum due to low population of triplet state at given temperature was suppressed under the mono radical impurity spectrum. At the elevated temperature clear five line EPR spectrum for biradical was observed. These observations reminded us the very well-known Tschitschibabin's HC which also suffered from the absence of triplet EPR spectrum in solution as discussed above. So we planned to revisit the discrepancies on the ground state of Tschitschibabin's HC. Alike in Tschitschibabin's HC, the two spin centers in BPNO are separated by the same spacer molecule. The BPNO can serve as a stable heteroatom analogue of Tschitschibabin's HC.

We reanalyzed the crystal structures of Thiele's and Tschitschibabin's HC, reported by Montgomery *et al.*,¹⁵ with DFT calculations. While the Thiele's HC showed bond alterations in phenylene ring indicating quinoid form, the

Tschitschibabin's HC did not show significant difference in alternating bonds of the biphenyl. Most importantly the C-C' bond (1.448 Å) between the phenylene rings was 0.1 Å longer than the typical double bond average, but still shorter than the typical aryl-aryl single bond distance (1.493 Å) in biphenyls. The crystal structure data for Tschitschibabin's HC recorded at three different temperatures did not show systematic change in bond lengths and dihedral angles.¹⁵ The DFT calculations were performed with the geometry of single crystal structure to obtain the singlet-triplet energy gap and to compare the spin density distribution. The estimated antiferromagnetic singlet-triplet energy gap for Thiele's and Tschitschibabin's HC were -27.7 and -8.1 kcal mol⁻¹ respectively using unrestricted broken symmetry (BS) B3LYP/6-31g(d) level of theory. Interestingly, while the $\langle S^2 \rangle$ values for BS-solution of Thiele's HC converges to zero, it was close to 1 ($\langle S^2 \rangle = 0.77$) for Tschitschibabin's HC. This clearly indicates the ground state of Thiele's and Tschitschibabin's HC is closed shell singlet and open shell singlet, respectively. The singlet-triplet energy gap for Tschitschibabin's HC was nearly double than that of BPNO, which suggested alike BPNO, Tschitschibabin's HC may also exist in semi-quinoid form. Therefore considering the very strong antiferromagnetic exchange interactions no significant population of triplet state occurs at room temperature or lower temperatures. So the triplet EPR spectrum of Tschitschibabin's HC was masked under monoradical impurities. If this hypothesis is true then all the historical discrepancies related to EPR spectra of Tschitschibabin's HC can be well accounted for.



Scheme 1. Synthesis of (a) BPNO and TPNO, and (b) BPTMP.

Thus to confirm our hypothesis, we designed and studied a series of phenylene bridged bisnitroxide molecules (Figure 3) experimentally as well as theoretically. The structure of PHNO (p-phenylenebis(N-*tert*-butylaminoxyl)) was comparable to Thiele's HC, both of which exist in a complete quinoid form. On further extending the π -bridge from monophenylene to biphenylene and terphenylene, molecules showed the transition from complete quinoid to complete biradicaloid form via semi-quinoid structure. Unlike Tschitschibabin's HC, excellent stability of the BPNO allowed its analysis under very harsh condition. In BPTMP (N,N'-((4,5,9,10-tetramethoxyppyrene-2,7-diyl)bis(4,1-phenylene))bis(N-(*tert*-butylaminoxyl))) the spacer molecule biphenyl tetramethoxyppyrene can be considered as a tetraphenylene in which two central phenyl rings are locked from the rotation.

Synthesis

In 1998 Iwamura *et al.* reported the synthesis and characterization of PHNO.³¹ The PHNO was analyzed by NMR, EPR, UV-Vis and single crystal X-ray analysis. Single crystal structure analysis revealed that PHNO exist in quinoid form which was supported by its EPR silence and clear NMR spectrum with two sharp singlets at 7.40 and 1.68 ppm. The UV-Vis spectrum of PHNO in DCM showed the broad absorption at 403 nm due to quinoid form. The BPNO and TPNO (N,N'-([1,1':4',1''-terphenyl]-4,4''-diyl)bis(N-(*tert*-butylaminoxyl))) were synthesized in two steps from corresponding 4,4'-dibromobiphenyl and 4,4'-dibromoterphenyl, respectively. As shown in Scheme 1a in first step the dibromo derivatives were lithiated with n -BuLi at -78

$^\circ\text{C}$ followed by addition of 2-methyl-2-nitrosopropane (*t*-BuNO) dimer, which gave bishydroxylamine (1 or 2). In second step oxidation of bishydroxylamine with Ag_2O in dichloromethane afforded the desired product BPNO or TPNO.³⁰ The Suzuki coupling reaction of 2,7-diiodo-4,5,9,10-tetramethoxyppyrene (3) and 4-(*tert*-butyl(*tert*-butyldimethylsilyloxy)-amino)phenyl-boronic acid (4PBA) gave the *tert*-butyldimethylsilyl protected bis(N-(*tert*-butyl)-N-phenylhydroxylamine) (4).^{29,32,33} The deprotection of the silyl group and subsequent oxidation of the obtained bishydroxylamine yielded BPTMP.³⁴

UV-Vis analysis

The UV-Vis spectra of BPNO and TPNO recorded in toluene at room temperature were completely different (Figure 4a & 4b). While the TPNO showed typical polyphenylene absorption at 349 nm with shoulder at 430 nm due to $n-\pi^*$ transition of *tert*-butylaminoxyl radical moiety, the BPNO displayed biphenyl absorption at 322 nm along with additional very strong absorption at 476 nm and weak absorption at 649 nm. As it has been found in previous studies^{30, 31} the two additional absorption peaks in BPNO at 476 nm and 649 nm which were completely absent in TPNO can be assigned to the presence of partial quinoid form. The BPTMP exhibited the pyrene absorption peak at 357 nm and low intensity broad absorption shoulder due to $n-\pi^*$ transition of radical moiety between 450 nm to 650 nm (Figure 4c). To probe into structural change with temperature, the BPNO in toluene was subjected to variable temperature (VT) UV-Vis measurements. Interestingly upon increasing the temperature the absorption peaks at 476 nm

and 649 nm due to quinoid form decreased and the absorption peak at 322 nm corresponding to benzenoid biphenyl core increased (Figure 5a). The hyperchromic shift of absorption band at 476 nm with temperature was analyzed applying the Arrhenius equation (Figure 5b).

$$\text{Arrhenius Equation, } K_{eq} = K \exp\left(-\frac{\Delta E_a}{k_B T}\right)$$

Where K_{eq} is the equilibrium constant, ΔE_a is the activation energy for the structural transformation, and k_B is the Boltzmann constant. The best Arrhenius fit gave the activation energy of 2.5 kcal mol⁻¹ for the structural transformation from semi-quinoid to benzenoid form (and vice-versa, Scheme 2).

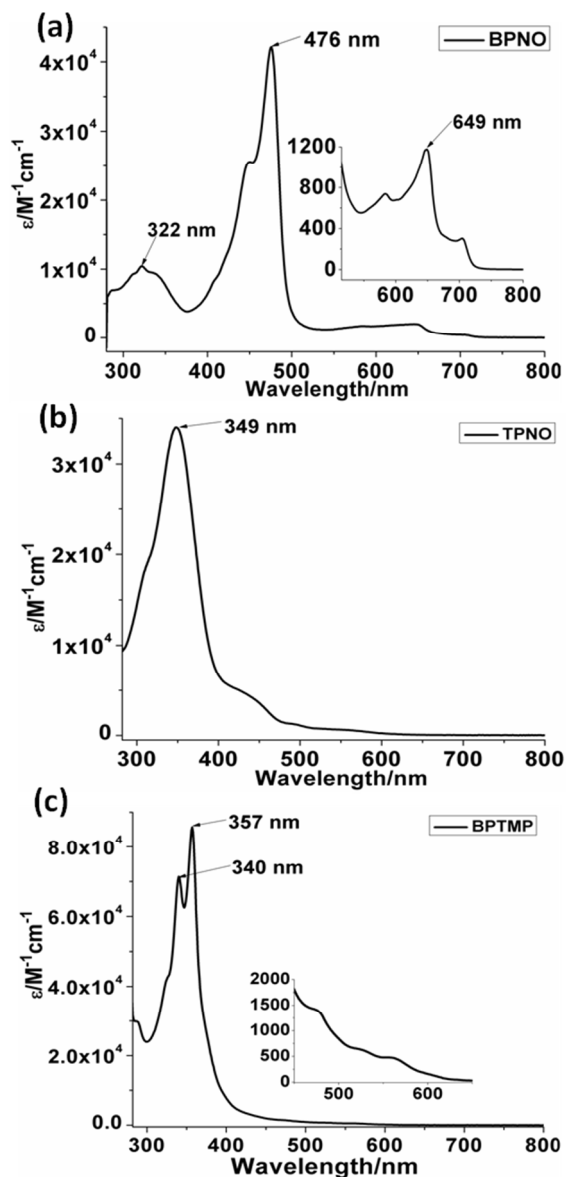


Figure 4. UV-Vis spectra of (a) BPNO (b) TPNO, and (c) BPTMP at room temperature in toluene.

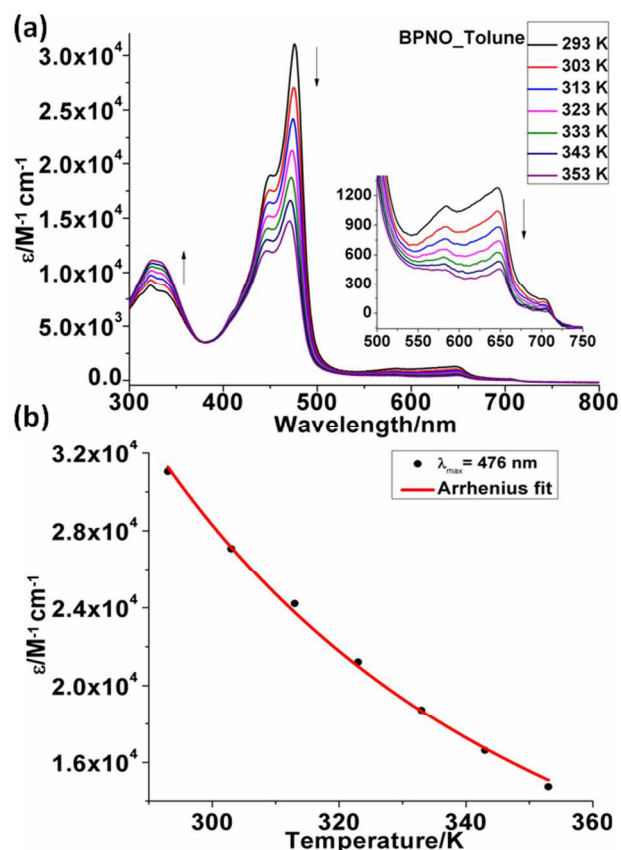
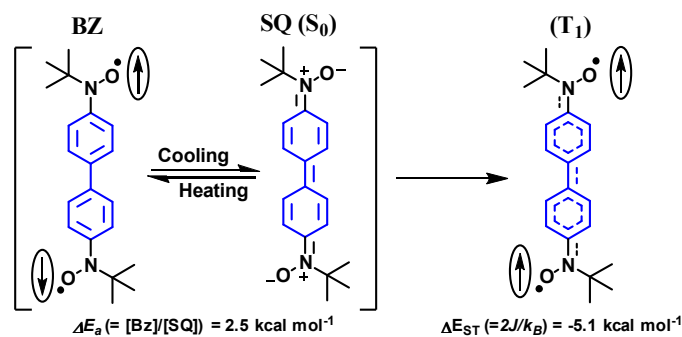


Figure 5. (a) Variable temperature UV-Vis spectra of BPNO in toluene, (b) change in absorption maxima (black dot) at 476 nm and Arrhenius fit (red line).



Scheme 2. Structural transformation with temperature.

EPR spectroscopy

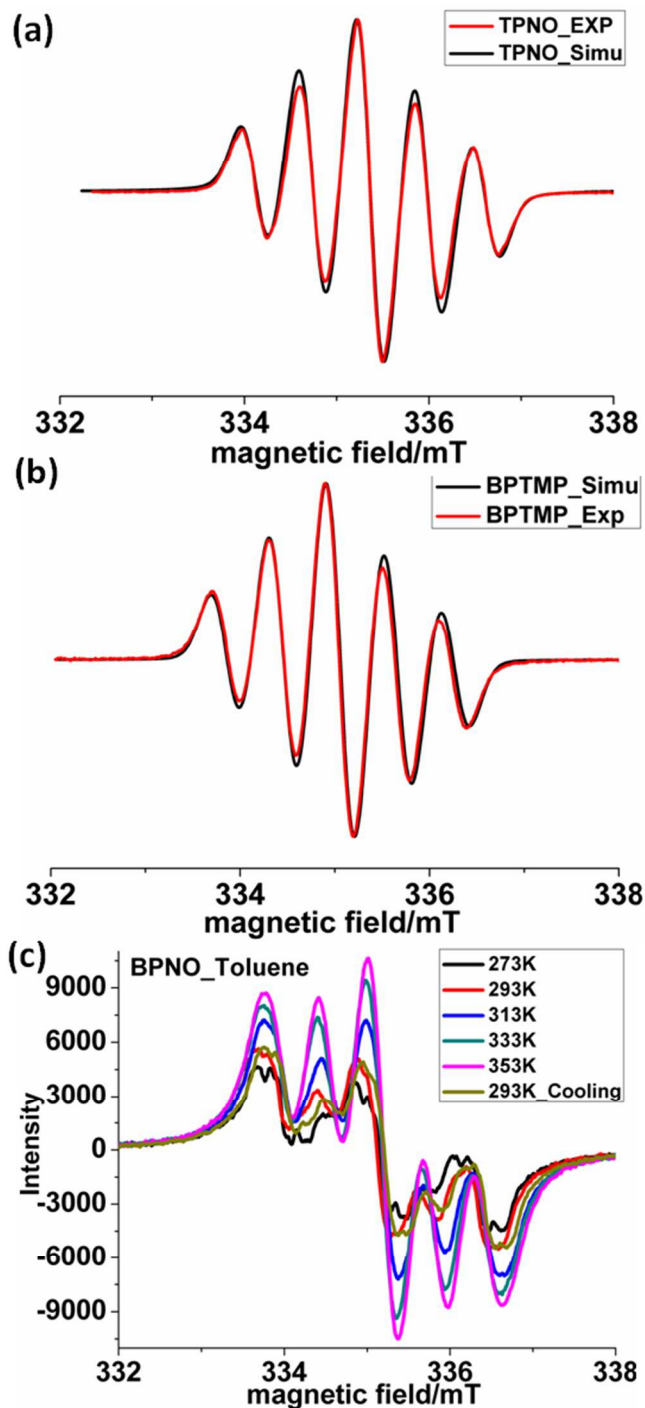


Figure 6. Experimental and simulated EPR spectra of (a) TPNO (parameters for spectral simulation: microwave frequency = 9.4195 GHz, lorentzian/gaussian = 0.5, line width = 3.2 G, $a_N/2 = 6.225$ G, $g = 2.0065$) and (b) BPTMP (parameters for spectral simulation: microwave frequency = 9.4108 GHz, lorentzian/gaussian = 0.5, line width = 3.0 G, $a_N/2 = 5.948$ G, $g = 2.0058$) in toluene at room temperature. (c) Variable temperature EPR spectra of BPNO in toluene.

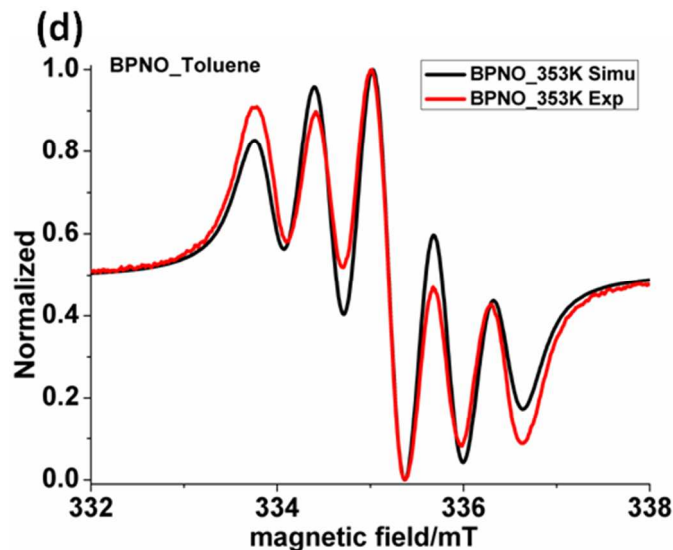


Figure 6. (d) Experimental and simulated EPR spectra of BPNO at 353 K in toluene (parameters for spectral simulation: microwave frequency = 9.4157 GHz, lorentzian/gaussian = 0.1, line width = 3.8 G, $a_N/2 = 6.250$ G, $g = 2.0067$).

The TPNO and BPTMP in toluene at room temperature gave typical five line EPR spectra for the biradical possessing two aminoxyl radical moieties (Figure 6a & 6b). The EPR spectra can be reproduced by spectral simulation considering two equivalent nitrogen hyperfine coupling constants $a_N/2 = 6.225$ G at $g = 2.0065$ for TPNO and $a_N/2 = 5.948$ G at $g = 2.0058$ for BPTMP. This demonstrates the exchange interactions J between radical moieties are much larger than the hyperfine coupling ($J \gg a_N$).³⁵ In contradiction to this the room temperature (293 K) EPR spectrum of BPNO in toluene appeared more alike mono radical species consisting of low intensity three lines with tiny shoulders in between as shown in Figure 6c. When this toluene solution of BPNO was subjected to VT EPR measurement these tiny shoulders became more predominant with increasing the temperature. Notably at 333 K clear five line spectrum for biradical was observed which became more prominent at 353 K. The detected spectrum at 353 K was recreated with spectral simulation taking two equivalent nitrogen hyperfine coupling constant $a_N/2 = 6.250$ G at $g = 2.0067$ (Figure 6d). The temperature dependent process was reversible as upon cooling the sample to 293 K the spectrum reached back to its previous position. The initially observed three line low intensity spectrum at room temperature may arise from the trace amount of mono radical impurity.

Furthermore a single crystal of BPNO was EPR active indicating that the sample is not in complete quinoid form in solid state. Notably with raising the temperature the signal intensity increased significantly showing inverse Curie like behavior thereby enhancing the paramagnetic content (Figure 7a). The increased signal intensity with temperature can be imputed to enhanced population of the triplet state. This is in accordance with the VT EPR and UV-Vis measurements in toluene which showed the increase in biradical nature of BPNO with raising the temperature. The temperature dependence of EPR signal intensity (Figure 7b) was analyzed using the Bleaney and Bowers equation as shown below.³⁶

$$I = 3(C/T) \exp\left(-\frac{\Delta E_{ST}}{k_B T}\right) / (1 + 3 \exp\left(-\frac{\Delta E_{ST}}{k_B T}\right))$$

The estimated singlet-triplet energy gap was as large as -5.1 kcal mol $^{-1}$. Therefore very strong antiferromagnetic exchange interactions are operating between two radical moieties in BPNO. Because of the large singlet-triplet energy gap very small population of triplet state occurs at room temperature which is in concomitance with the low intensity EPR spectrum in toluene at room temperature. All these experimental results led to the inference that BPNO exists in semi-quinoid form and exhibits structural transformation with temperature. While at low temperature it shows more quinoid character at higher temperature it stabilizes in biradicaloid form (Scheme 2). To collect more information about the structure of these molecules the single crystals were obtained and their structures compared.

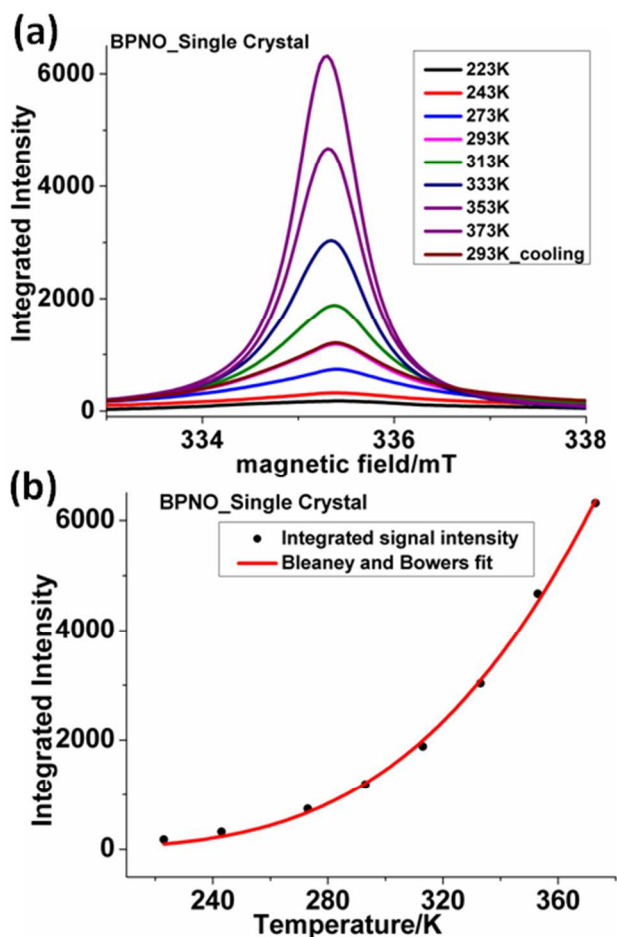


Figure 7. (a) Integrated EPR spectra of single crystalline BPNO at different temperature and (b) change in integrated signal intensity with temperature (black dot) and Bleaney and Bowers fit (red line).

Crystal structure analysis

The crystal structure analysis was a vital requirement to get an insight into structure of molecules under study. Good quality crystals were grown by slow diffusion of hexane to the solution of samples in DCM. Single crystals were analyzed using single crystal X-ray diffraction method. For comparison purpose the single crystal structure for PHNO was obtained from CCDC on

request. Crystal structure analysis of PHNO indicated the presence of two independent molecules (PHNO1 and PHNO2) in an asymmetric unit. Although the bond lengths and dihedral angles differ slightly, both the molecules showed alternating C–C bond lengths where the aminoxy group was in plane with the benzene ring. The N–O bond was slightly elongated and C–N bond was shortened (Table 1) in comparison with typical C–N (1.41 Å) and N–O (1.27 Å) bond lengths in phenyl aminoxy. Thus the structure of PHNO was concluded as the one of the quinoid form. So far the UV-Vis and EPR analysis indicated that while TPNO and BPTMP were in complete biradicaloid form, the BPNO exists in semi-quinoid form. Thus it was intriguing to compare the crystal structure of BPNO with completely quinoid form PHNO and wholly biradicaloid form TPNO (or BPTMP). Crystal structure analysis of TPNO and BPTMP revealed the C–N bond length was larger (distinctive of C–N single bond) in comparison to PHNO. The C–C bond lengths were of the order of typical C–C bond of phenylenes. The aminoxy radical moiety formed a dihedral angle of 28° and 20° with respect to the phenyl ring in TPNO and BPTMP respectively. The dihedral angle between central and terminal phenyl ring of TPNO was 15°. Crystal structure analysis of BPNO indicated that the two phenyl rings were nearly coplanar with each other (dihedral angle 0.2°) and the aminoxy group was slightly deviated from the plane of phenyl ring with dihedral angle of 7°. The C–N bond length in BPNO was larger than the PHNO but comparable to TPNO and BPTMP. The C–C bond length (1.458 Å) between two phenyl ring of BPNO was comparable to Tschitschibabin's HC (1.448 Å) but slightly shorter in comparison with TPNO (1.481 Å). Further the major difference in the structure of BPNO and TPNO came from the planarity of phenyl ring with respect to each other and the planarity of aminoxy group with respect to the phenyl ring. The planarity of phenyl rings and aminoxy group in BPNO gave better overlap of π -orbitals in comparison to TPNO. Thus even though the bond lengths were comparable in BPNO and TPNO, the BPNO exists in semi-quinoid form owing to the exceptional planarity.

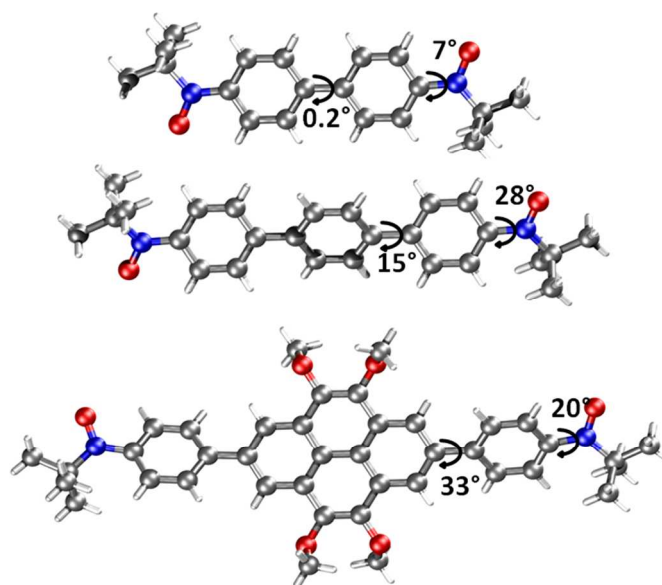
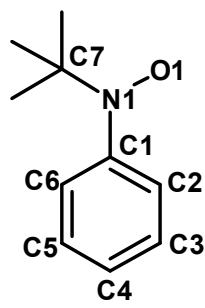


Figure 8. Single crystal structure of BPNO, TPNO, and BPTMP.

Table 1. Selected bond lengths and bond angles.

		PHNO1	PHNO2	BPNO	TPNO	BPTMP	
bond lengths/Å		1.291	1.287	1.284	1.290	1.272	
		N1–C1	1.354	1.362	1.411	1.413	1.422
		C1–C2	1.423	1.417	1.406	1.401	1.399
		C2–C3	1.362	1.358	1.380	1.387	1.399
dihedral angle/°							
O1–N1–C1–C2		1.2	3.4	7.0	28.0	20.3	

Theoretical calculations

To examine the biradical character of ground state (S_0) of molecules, HF and DFT calculations were performed using the crystal structure geometries.³⁷ Initially the degree of biradical character (y) was predicted by simple two-electron two-orbital model using the occupation numbers of the unrestricted non-bonding orbitals (UNOs) of UHF/6-31g(d, p) as proposed by Kamada *et al.*^{38, 39} The biradical character obtained from these calculations has value between 0 and 1, which corresponds to closed shell and pure biradical system respectively.

$$y = 1 - \frac{4(\sigma_{HOMO} - \sigma_{LUMO})}{4 + (\sigma_{HOMO} - \sigma_{LUMO})^2}$$

The theoretical value of y can be calculated from the occupation numbers of frontier orbitals, σ_{HOMO} and σ_{LUMO} , using the equation shown above. The estimated values of degree of biradical character, y , for Thiele's and Tschitschibabin's HC are 0.31 and 0.72 respectively which clearly indicates that while the former has closed shell structure the latter has more biradicaloid structure but relatively lower than the ideal biradical system. In a similar way the degree of biradical character increases on moving from PHNO to TPNO (Table 2). TPNO which showed the clear biradical EPR spectrum at room temperature has biradical character (0.99) close to the theoretical value (1.00) of pure biradical system. It should be noted that for the completely quinoid molecule PHNO slight over estimation of y value was observed with HF calculations. Thus to investigate further the broken symmetry DFT approach proposed by Noodleman *et al.* was employed to evaluate the energy difference between ground state (S_0) and triplet state (T_1).⁴⁰ The singlet-triplet energy gap was calculated with the generalized spin projection method suggested by Yamaguchi *et al.*⁴¹⁻⁴³

$$\Delta E_{ST} = \frac{(E(BS) - E(T))}{(S^2(T) - S^2(BS))} * 2$$

Where $E(BS)$ and $E(T)$ are the energies of the broken symmetry singlet and triplet state, respectively, and $\langle S^2 \rangle$ are the spin operator for these states. As shown in Table 2 the triplet T_1

state is always higher in energy than the singlet S_0 state. The $\langle S^2 \rangle$ values of BS calculation converge to zero for the closed shell structures Thiele's HC and PHNO. Interestingly, the $\langle S^2 \rangle$ values of BS-solution for pure biradicals TPNO and BPTMP are 0.98 and 1.00, respectively, as anticipated for singlet ground state biradicals, and do not converge to zero but close to one for Tschitschibabin's HC ($\langle S^2 \rangle = 0.81$) and BPNO ($\langle S^2 \rangle = 0.76$). This designates the S_0 state of Tschitschibabin's HC and BPNO is open shell singlet. Using BS-DFT more precise information about the ground state of molecules under investigation was obtained. The singlet-triplet energy difference decreases rapidly with increasing the length of the π -spacer. The calculated singlet-triplet energy gap for BPNO using BS-DFT calculations ($-4.9 \text{ kcal mol}^{-1}$) is well in accordance with the estimated value ($-5.1 \text{ kcal mol}^{-1}$) from the VT EPR measurement. The T_1 state population obtained using Boltzmann distribution and the energy gaps are 0.06 % and 0.0004 % for BPNO and Tschitschibabin's HC respectively.

To get an additional insight into the nature of open shell compounds, the frontier molecular orbitals were investigated. As shown in Figure 9 for the pure biradical system TPNO and BPTMP the SOMOs are confined on either half of the molecule with nearly no overlap between them.^{44, 45} As the two unpaired electrons in two SOMOs reside on different part of the molecule, TPNO and BPTMP can be classified as singlet disjoint biradicals.^{46, 47} In contrast, the SOMOs of Tschitschibabin's HC and BPNO are no longer confined separately but overlap at the center of the molecules which takes them little away from the class of the disjoint singlet biradicals. Interestingly while the spin density of triplet state is highly delocalized in Tschitschibabin's HC and BPNO, it is more located on the radical moiety than the phenyl rings in TPNO. In case of BPTMP the triplet spin density is more localized on terminal phenyl ring and radical moiety, with only minor contribution at the pyrene core.

Table 2. Summary of DFT calculations.

Molecule	E/eV (Triplet)	$\langle S^2 \rangle$ (triplet)	E/eV (BS-Singlet)	$\langle S^2 \rangle$ (BS)	$\Delta E_{ST}/$ kcal mol ⁻¹	Biradical character (γ) ^c
Thiele's HC	-33566.36324	2.023	-33567.58100	0.00	-27.75 ^a	0.31
Tschitschibabin's HC	-39836.20305	2.039	-39836.41784	0.81	-8.11 ^a	0.72
PHNO1	-21927.01325	2.003	-21927.67049	0.00	-15.16 ^b	0.60
PHNO2	-21928.54546	2.000	-21929.24631	0.00	-16.16 ^b	0.57
BPNO	-28209.51581	2.006	-28209.6485	0.76	-4.91 ^b	0.85
TPNO	-34494.35992	2.008	-34494.37674	0.98	-0.75 ^b	0.99
BPTMP	-57379.63065	2.008	-57379.63317	1.00	-0.12 ^b	-

^acalculated at UB3LYP/6-31g(d) level, ^bcalculated at UBLYP/6-31g(d) level, ^ccalculated at UHF/6-31g(d, p) level.

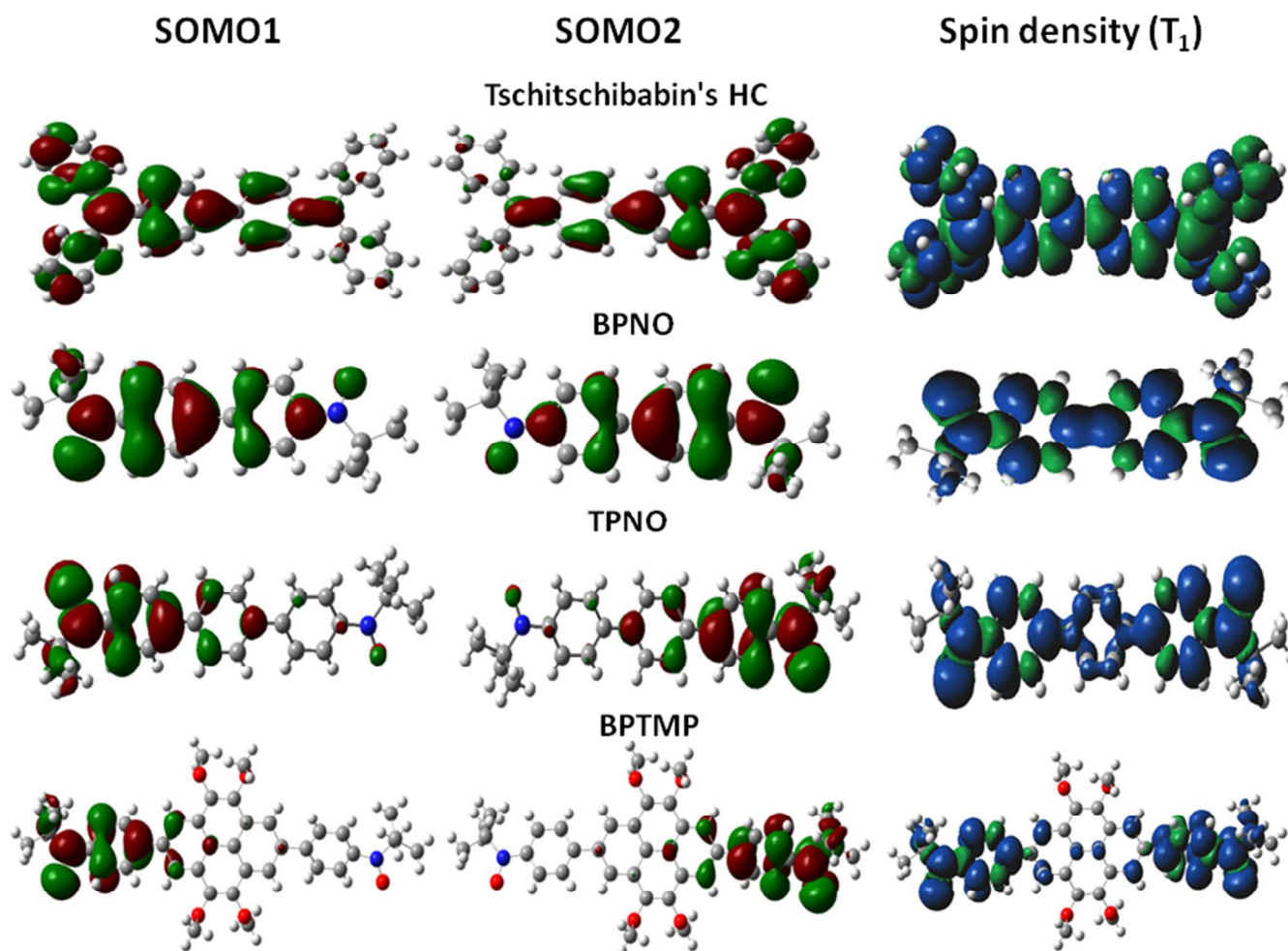


Figure 9. Calculated SOMOs of BS singlet and spin density distribution of triplet state.

Conclusion

In summary the serendipitous synthesis of BPNO, the open shell singlet semi-quinoid molecule, led us to dig the discrepancies related to Tschitschibabin's HC. For the better understanding of the transition from the purely quinoid to pure biradicaloid structure via the semi-quinoid form a series of molecules with extended π -bridge are compared and analyzed. While the longer extended molecules TPNO ($r_{N-N} = 1.43$ nm) and BPTMP ($r_{N-N} = 1.84$ nm) showed clear biradical features at room temperature with 5 line EPR spectra where $J \gg a_N$, the BPNO ($r_{N-N} = 1.0$ nm) is a borderline case best described as semi-quinoid. Combining all the theoretical and experimental results led to the inference that like BPNO the Tschitschibabin's HC also possess the semi-quinoid structure with very strong antiferromagnetic exchange interactions. Because of this very small population of triplet state (< 0.1 %) occurs at room temperature, leading to weak intensity triplet EPR spectrum which can be masked under even ~ 0.1 % impurity of mono radical species thereby giving doublet like spectrum. Furthermore the poor stability of Tschitschibabin's HC under ambient conditions may not allow its unquestionable spectroscopic analysis at elevated temperature as there is possibility of thermal decomposition. The exceptional stability of BPNO permitted its analysis by UV-Vis and EPR at higher temperatures. The VT EPR measurements clearly showed that the small population of triplet state becomes significant at higher temperature. Therefore in conclusion alike BPNO the Tschitschibabin's HC can also be classified as the new class of molecules which exist in semi-quinoid form and exhibit the property of biradical and quinoid form simultaneously. Moreover these analyses can help in the better understanding of the biradical character of recently pushed search for singlet open shell polyaromatic HCs.

Acknowledgement

A Support from SFB-TR49 and a scholarship for P.R. are gratefully acknowledged.

Address

Max Planck Institute for Polymer Research, Ackermannweg 10, 55128 Mainz, Germany.

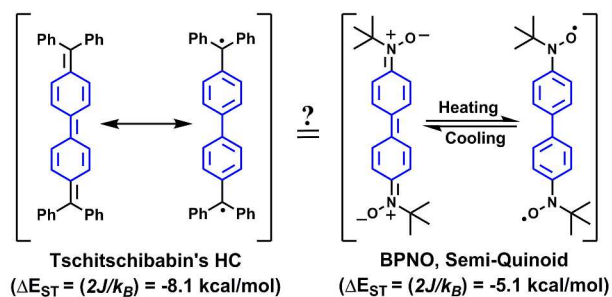
Electronic Supplementary Information (ESI) available: [Detailed experimental procedures, crystallographic table and ORTEP diagrams]. See DOI: 10.1039/b000000x/

Notes and References

- M. Gomberg, *J. Am. Chem. Soc.*, 1900, **22**, 757-771.
- A. E. Tschitschibabin, *Chem. Ber.*, 1907, **40**, 1810-1819.
- T. Sugawara and M. M. Matsushita, *J. Mater. Chem.*, 2009, **19**, 1738-1753.
- S. A. Wolf, D. D. Awschalom, R. A. Buhrman, J. M. Daughton, S. von Molnár, M. L. Roukes, A. Y. Chtchelkanova and D. M. Treger, *Science*, 2001, **294**, 1488-1495.
- Y. Morita, S. Suzuki, K. Sato and T. Takui, *Nat. Chem.*, 2011, **3**, 197-204.
- Z. Sun, Z. Zeng and J. Wu, *Chem. Asian J.*, 2013, **8**, 2894-2904.
- A. Ueda, S. Suzuki, K. Yoshida, K. Fukui, K. Sato, T. Takui, K. Nakasuji and Y. Morita, *Angew. Chem. Int. Ed.*, 2013, **52**, 4795-4799.
- A. Shimizu, T. Kubo, M. Uruichi, K. Yakushi, M. Nakano, D. Shiomi, K. Sato, T. Takui, Y. Hirao, K. Matsumoto, H. Kurata, Y. Morita and K. Nakasuji, *J. Am. Chem. Soc.*, 2010, **132**, 14421-14428.
- Z. Zeng, Y. M. Sung, N. Bao, D. Tan, R. Lee, J. L. Zafra, B. S. Lee, M. Ishida, J. Ding, J. T. López Navarrete, Y. Li, W. Zeng, D. Kim, K.-W. Huang, R. D. Webster, J. Casado and J. Wu, *J. Am. Chem. Soc.*, 2012, **134**, 14513-14525.
- X. Zheng, X. Wang, Y. Qiu, Y. Li, C. Zhou, Y. Sui, Y. Li, J. Ma and X. Wang, *J. Am. Chem. Soc.*, 2013.
- A. Konishi, Y. Hirao, M. Nakano, A. Shimizu, E. Botek, B. Champagne, D. Shiomi, K. Sato, T. Takui, K. Matsumoto, H. Kurata and T. Kubo, *J. Am. Chem. Soc.*, 2010, **132**, 11021-11023.
- C. Lambert, *Angew. Chem. Int. Ed.*, 2011, **50**, 1756-1758.
- D. C. Reitz and S. I. Weissman, *J. Chem. Phys.*, 1960, **33**, 700-704.
- J. Thiele and H. Balhorn, *Chem. Ber.*, 1904, **37**, 1463-1470.
- L. K. Montgomery, J. C. Huffman, E. A. Jurczak and M. P. Grendze, *J. Am. Chem. Soc.*, 1986, **108**, 6004-6011.
- H. M. McConnell, *J. Chem. Phys.*, 1960, **33**, 1868-1869.
- H. Hartmann, H. D. Brauer and H. Schafer, *Zeitschrift Fur Physikalische Chemie-Frankfurt*, 1968, **61**, 119-&.
- H. D. Brauer, H. Stieger and H. Hartmann, *Zeitschrift Fur Physikalische Chemie-Frankfurt*, 1969, **63**, 50-&.
- F. Popp, F. Bickelhaupt and C. Maclean, *Chem. Phys. Lett.*, 1978, **55**, 327-330.
- L. K. Montgomery, J. C. Huffman, E. A. Jurczak and M. P. Grendze, *J. Am. Chem. Soc.*, 1986, **108**, 6004-6011.
- H. M. McConnell, *J. Chem. Phys.*, 1960, **33**, 115-121.
- C. A. Hutchison, A. Kowalsky, R. C. Pastor and G. W. Wheland, *J. Chem. Phys.*, 1952, **20**, 1485-1486.
- H. Stieger and H. D. Brauer, *Chem. Ber. Recl.*, 1970, **103**, 3799-&.
- Y. Kanzaki, D. Shiomi, K. Sato and T. Takui, *J. Phys. Chem. B*, 2012, **116**, 1053-1059.
- H. D. Brauer, H. Stieger, J. S. Hyde, L. D. Kispert and Luckhurs, *Mol. Phys.*, 1969, **17**, 457-&.
- W. J. van der Hart and L. J. Oosterhoff, *Mol. Phys.*, 1970, **18**, 281-284.
- P. Ravat, Y. B. Borozdina, Y. Ito, V. Enkelmann and M. Baumgarten, *Cryst. Growth Des.*, 2014, **14**, 5840-5846.
- Y. B. Borozdina, E. Mostovich, V. Enkelmann, B. Wolf, P. T. Cong, U. Tutsch, M. Lang and M. Baumgarten, *J. Mater. Chem. C*, 2014, **2**, 6618-6629.
- P. Ravat, Y. Ito, E. Gorelik, V. Enkelmann and M. Baumgarten, *Org. Lett.*, 2013, **15**, 4280-4283.
- P. Ravat, Y. Teki, Y. Ito, E. Gorelik and M. Baumgarten, *Chem. Eur. J.*, 2014, **20**, 12041-12045.
- S. Nakazono, S. Karasawa, N. Koga and H. Iwamura, *Angew. Chem. Int. Ed.*, 1998, **37**, 1550-1552.
- R. J. Smith and R. M. Pagni, *J. Org. Chem.*, 1981, **46**, 4307-4309.
- J. C. Stowell, *J. Org. Chem.*, 1971, **36**, 3055-3056.
- P. Ravat, T. Marszalek, W. Pisula, K. Müllen and M. Baumgarten, *J. Am. Chem. Soc.*, 2014, **136**, 12860-12863.
- M. Shinomiya, K. Higashiguchi and K. Matsuda, *J. Org. Chem.*, 2013, **78**, 9282-9290.
- B. Bleaney and K. D. Bowers, *Proc. R. Soc. London A*, 1952, **214**, 451-465.
- G. W. T. M. J. Frisch, H. B. Schlegel, G. E. Scuseria, M. A. Robb, J. R. Cheeseman, G. Scalmani, V. Barone, B. Mennucci, G. A. Petersson, H. Nakatsuji, M. Caricato, X. Li, H. P. Hratchian, A. F. Izmaylov, J. Bloino, G. Zheng, J. L. Sonnenberg, M. H. A. F. Izmaylov, J. Bloino, G. Zheng, J. L. Sonnenberg, M. Hada, M. Ehara, K. Toyota, R. Fukuda, J. Hasegawa, M. Ishida, T. Nakajima, Y. Honda, O. Kitao, H. Nakai, T. Vreven, J. A. Montgomery, Jr., J. E. Peralta, F. Ogliaro, M. Bearpark, J. J. Heyd, E. Brothers, K. N. Kudin, V. N. Staroverov, R. Kobayashi, J. Normand, K. Raghavachari, A. Rendell, J. C. Burant, S. S. Iyengar, J. Tomasi, M. Cossi, N. Rega, J. M. Millam, M. Klene, J. E. Knox, J. B. Cross, V. Bakken, C. Adamo, J. Jaramillo, R. Gomperts, R. E. Stratmann, O. Yazyev, A. J. Austin, R. Cammi, C. Pomelli, J. W. Ochterski, R. L. Martin, K. Morokuma, V. G. Zakrzewski, G. A. Voth, P. Salvador, J. J. Dannenberg, S. Dapprich, A. D. Daniels, O. Farkas, J. B. Foresman, J. V. Ortiz, J. Cioslowski, and D. J. Fox., in *Gaussian 09*, Gaussian, Inc, Wallingford CT, 2009.
- K. Kamada, K. Ohta, A. Shimizu, T. Kubo, R. Kishi, H. Takahashi, E. Botek, B. Champagne and M. Nakano, *J. Phys. Chem. Lett.*, 2010, **1**, 937-940.
- P. O. Dral and T. Clark, *J. Phys. Chem. A*, 2011, **115**, 11303-11312.
- L. Noodleman, *J. Chem. Phys.*, 1981, **74**, 5737-5743.

41. K. Yamaguchi, F. Jensen, A. Dorigo and K. N. Houk, *Chem. Phys. Lett.*, 1988, **149**, 537-542.
42. T. Soda, Y. Kitagawa, T. Onishi, Y. Takano, Y. Shigeta, H. Nagao, Y. Yoshioka and K. Yamaguchi, *Chem. Phys. Lett.*, 2000, **319**, 223-230.
43. M. Shoji, K. Koizumi, Y. Kitagawa, T. Kawakami, S. Yamanaka, M. Okumura and K. Yamaguchi, *Chem. Phys. Lett.*, 2006, **432**, 343-347.
44. A. D. Becke, *J. Chem. Phys.*, 1993, **98**, 1372-1377.
45. E. R. Davidson and D. Feller, *Chem. Rev.*, 1986, **86**, 681-696.
46. W. T. Borden, H. Iwamura and J. A. Berson, *Acc. Chem. Res.*, 1994, **27**, 109-116.
47. W. T. Borden and E. R. Davidson, *J. Am. Chem. Soc.*, 1977, **99**, 4587-4594.
48. S.-i. Kawano, M. Baumgarten, D. Chercka, V. Enkelmann and K. Müllen, *Chem. Commun.*, 2013, **49**, 5058-5060.

TOC Graphics



Revisiting the history: Towards the better understanding of open shell singlet biradicaloids.